Stress-Strain Characteristics in Ni-Ga-Fe Ferromagnetic Shape Memory Alloys

Stress-strain characteristics in Ni–Ga–Fe ferromagnetic shape memory alloys

Y. Sutou, N. Kamiya, T. Omori, R. Kainuma, and K. Ishida[a)]
Department of Materials Science, Graduate School of Engineering, Tohoku University, Aoba-yama 02, Sendai 980-8579, Japan

K. Oikawa
National Institute of Advanced Industrial Science and Technology, 4-2-1 Nigatake, Miyagino-ku, Sendai 983-8551, Japan

(Received 19 May 2003; accepted 26 November 2003)

Tensile and compressive stress–strain characteristics for Ni–Ga–Fe ferromagnetic shape memory alloys at several temperatures were investigated by mechanical test and a critical stress versus temperature diagram was obtained. The crystal structure of the martensite phase obtained by tensile-stress-induced martensitic transformation was estimated from the degree of the transformation strain. Stress-induced martensite transformed from the parent phase with an $L2_1$ structure showed a 14M structure by tensile stress and by further applying stress, the 14M structure martensitically was transformed into an $L1_0$ structure. Moreover, it was found in the compressive test that variant rearrangement occurred by very low compressive stress less than 3 MPa, which is similar to the phenomenon seen in Ni–Mn–Ga alloys. © *2004 American Institute of Physics.* [DOI: 10.1063/1.1642277]

Ferromagnetic shape memory alloys (FSMAs) such as Ni–Mn–Ga,[1] Fe–Pd,[2] Fe–Pt,[3] Ni–Mn–Al,[4,5] Co–Ni–Ga,[6] and Co–Ni–Al[7,8] are drawing strong attention as a new class of magnetically controlled actuator materials. They show a large magnetic-field-induced strain (MFIS) due to the variant rearrangement in the martensite phase. Especially in the Ni–Mn–Ga FSMAs, giant MFISs of 6% and 9.5% in the martensite phase with a five-layered and a seven-layered modulated structure, respectively, have been reported.[9] However, the Ni–Mn–Ga single crystals fabricated by the Bridgman method show significant macroscopic segregation of Ni and Mn in the direction of growth of the crystal and the overall compositions in the grown crystal shift from the nominal ones, which is caused by the loss of Mn due to evaporation.[10]

Recently, Oikawa *et al.* have found the Ni–Ga–Fe alloys to be a promising FSMA candidates.[11,12] According to their study, the parent phase with the B2 and/or the $L2_1$ structure martensitically transforms into a seven-layer modulated structure (14M) and a five-layer modulated (10M) structure upon cooling. More recently, some additional investigations have been reported.[13–15]

In the present study, the stress–strain characteristics in the parent and the martensite phases for Ni–Ga–Fe single-crystals were investigated by tensile and compressive testing, and very low compressive stress for variant rearrangement was obtained. Therefore, the possibility of the appearance of a large MFIS for Ni–Ga–Fe alloys can be expected.

The alloys $Ni_{54}Ga_{27}Fe_{19}$ and $Ni_{54.1}Ga_{26.9}Fe_{19}$ were prepared by induction melting under an argon atmosphere. The obtained ingots were cast in an alumina crucible and then single-crystal specimens 50 mm in length and 15 mm in diameter were grown in a Bridgman crystal growth furnace under an argon atmosphere. The single-crystal specimens were homogenized at 1170 °C for 1 day and then quenched in water. The crystallographic orientation of the high-temperature cubic phase ($L2_1$ structure) was determined by electron backscatter diffraction (EBSD). Single-crystal specimens for differential scanning calorimetric (DSC) measurement and tensile and compressive testing were cut by a spark-cutting machine. Finally, the specimens were wet polished and electropolished before the mechanical test.

Figure 1 shows the typical tensile stress–strain curves of a $Ni_{54}Ga_{27}Fe_{19}$ single crystal at several temperatures at a strain rate of 0.5 mm/min, where the size of the tensile specimen in the gauge-length portion was $2.0\times0.6\times15.0$ mm^3 and the tensile direction was an orientation of nearly ⟨100⟩ as indicated in the stereographic triangle inserted in Fig. 1(a). It was detected from DSC measurement that the martensitic transformation starts at $M_s=4.7$ °C and finishes at $M_f=0.2$ °C, and that the reverse transformation starts at

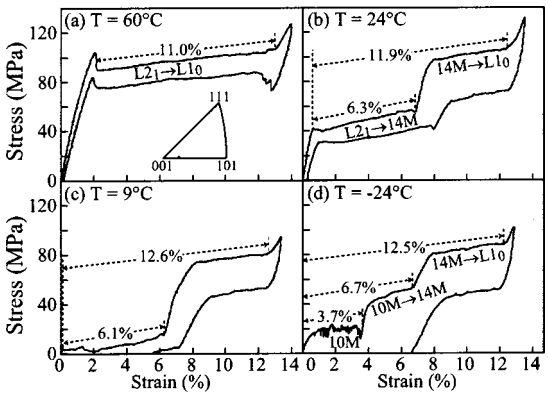

FIG. 1. Tensile stress–strain curves at (a) 60 °C, (b) 24 °C, (c) 9 °C, and (d) −24 °C for the $Ni_{54}Ga_{27}Fe_{19}$ single crystal: (a) shows the stereo triangle of the parent phase indicating the direction $\sim[105]_{L2_1}$ of the applied tensile stress.

a)Electronic mail: ishida@material.tohoku.ac.jp

TABLE I. Lattice parameters for each structure, the calculated transformation strain $\epsilon_{cal.}$ by using the lattice deformation and the observed transformation strain $\epsilon_{obs.}$ in tensile test shown in Fig. 1, where the lattice parameters of the martensite structure for 14M, 10M, and $L1_0$ were determined by assuming the lattice correspondence with the B2 parent structure.

		Transformation strain (%)								
		$\epsilon_{cal.}$				$\epsilon_{obs.}$				
	Lattice parameter	100	110	111	105	105				
Structure	(nm)					−49 °C	−24 °C	9 °C	24 °C	60 °C
$L2_1$(B2)	a_0=0.576 (0.288)									
10M[a]	a=0.424, b=0.269, c=2.088, β=91.49°	4.6	4.0	0.6	4.8	3.9	3.7			
14M	a=0.424, b=0.269, c=2.927, β=93.18°	6.2	4.0	0.6	6.2	6.2	6.7	6.1	6.3	
$L1_0$[b]	a=0.381, c=0.327	13.6	4.0	0.6	12.9	12.3	12.5	12.6	11.9	11.0

[a]Evaluated from the lattice parameter of the 14M structure by considering the stacking order of the 10M structure.

[b]Estimated from the 14M structure by using equations $a_{L1_0}=\sqrt{2}b_{14M}$ and $c_{L1_0}=\sqrt{a_{14M}^2-b_{14M}^2}$.

A_s=4.7 °C and finishes at A_f=9.6 °C. It can be seen from the stress–strain curves tested above A_f that the stress-induced martensitic transformation occurs by applying the tensile loading and that nearly perfect reverse transformation occurs with unloading as shown in Figs. 1(a) and 1(b). Figure 1(b) shows that the martensite phase stress induced from parent phase transforms into another phase by further tensile loading. This two-step transformation is considered to be a martensite-to-martensite transformation. At 9 °C in Fig. 1(c), although a two-step transformation due to loading is also observed, the initial stress-induced martensite phase remains after unloading because the testing temperature is near A_f. In the low temperature region under M_s, three plateaus appear and only the final stress-induced martensite phase reverse transforms by unloading as shown in Fig. 1(d). These two- and three-step transformations have also been reported for the Ni–Mn–Ga alloys.[16,17]

In order to estimate the kind of crystal structure of the stress-induced martensite phase, the transformation strains represented by the length of the plateaux of $L2_1$–10M, $L2_1$–14M, and $L2_1$–$L1_0$ transformations which were observed in the present Ni–Ga–Fe alloys calculated by using the lattice deformation.[18,19] The lattice parameters of the $L2_1$ and the 14M structures were obtained by x-ray diffraction and those of the 10M and $L1_0$ structures were estimated from the 14M structure by using methods reported in the references.[20,21] The lattice parameters used for the calculations are summarized in Table I, where the lattice parameters of the martensite structure were determined by assuming lattice correspondence with the B2 structure for the parent phase.

Table I lists the orientation dependence on the transformation strain $\epsilon_{cal.}$ in ⟨100⟩, ⟨110⟩, ⟨111⟩, and ⟨105⟩ tensile directions for each transformation and the observed strain $\epsilon_{obs.}$ of −49, −24, 9, 24, and 60 °C. The $\epsilon_{cal.}$ in the ⟨105⟩ tensile direction is the same as that of the tested specimen. It can be seen that the maximum transformation strain is obtained near the ⟨105⟩ tensile direction for the 10M and the 14M and in the ⟨100⟩ tensile direction for the $L1_0$, while very small transformation strain is obtained in the ⟨111⟩ tensile direction. It is deduced from the observed transformation strain $\epsilon_{obs.}$ that the martensite structure stress induced from $L2_1$ at 60 °C is the $L1_0$ and that the initial stress-induced martensite structure and the second one observed at 9 and 24 °C would be the 14M and the $L1_0$, respectively. At −49 and −24 °C, it is inferred from the observed strain $\epsilon_{obs.}$ that in the initial plateau region, the variant reorientation of the thermally induced martensite phase with the 10M structure proceeds due to the loading and that the 10–14M stress-induced transformation followed by the 14M–$L1_0$ stress-induced transformation subsequently occurs. From these results, the critical stress versus temperature diagram can be drawn as shown in Fig. 2. This kind of critical stress versus temperature diagram is very similar to that reported in the Cu–Al–Ni SMAs.[22] In the $Ni_{54}Ga_{27}Fe_{19}$ alloy, the 14M martensite is stress induced from the parent with the $L2_1$ structure and then the $L1_0$ martensite is stress induced from the 14M martensite by further tensile loading at temperatures between M_s and 40 °C. At above 40 °C, the $L1_0$ martensite may be directly stress induced from the parent with $L2_1$. One of the characteristic features of the stress–strain curve of this temperature region is that the stress drastically decreases just after the onset of the stress-induced martensitic transformation and then enters a steady state. If the highest critical stress is plotted in a critical stress versus temperature diagram, the critical stress indicated as the AB line exists on the extension line of the boundary for the $L2_1$–14M stress-induced transformation, while the lower stress indicated as the ac line should correspond to the critical stress for the stress-induced $L1_0$ structure. This suggests that the $L1_0$ structure cannot be directly stress induced from $L2_1$, being only stress induced from $L2_1$ via 14M. In other words, the habit plane which is the undistorted plane between $L2_1$ and 14M is more easily created than that between $L2_1$ and $L1_0$, because the 14M structure includes high density microtwins with an ordered stacking structure whose introduction would make the formation of an undistorted plane easy. On the other hand, at temperatures below M_s, three plateaus which correspond to the variant reorientation of the 10M and the 10–14M and the 14M–$L1_0$ transformations were observed as previously mentioned. It is noteworthy that three plateaus do not appear in the stress-induced transformation at temperatures above M_s, because the 10M martensite appears from the $L2_1$ only by thermal-induced transformation on

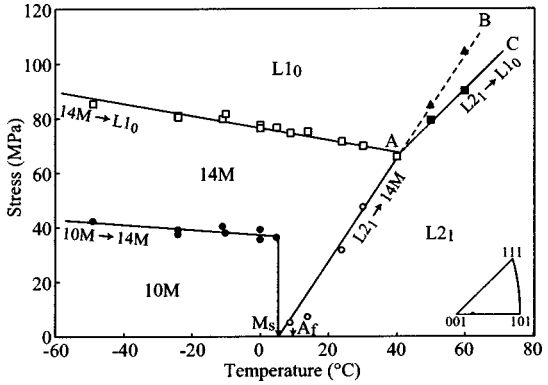

FIG. 2. Critical stress vs temperature diagram obtained from the tensile test in the $Ni_{54}Ga_{27}Fe_{19}$ single crystal. The inset shows the stereo triangle of the parent phase indicating the direction of the applied tensile stress.

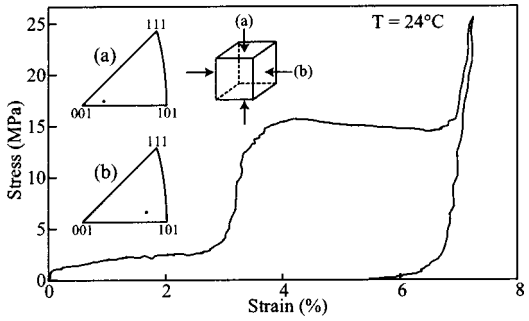

FIG. 3. Compressive stress–strain curves at 24 °C for the $Ni_{54.1}Ga_{26.1}Fe_{19}$ single crystal. The insets show the stereo triangle of the parent phase indicating the directions of the applied tensile stress; (a) predeformation direction, and (b) test direction.

cooling. Actually, it has been confirmed by transmission electron microscopy (TEM) that the $L2_1$ parent phase transforms into the 10M martensite phase upon cooling in the $Ni_{54}Ga_{27}Fe_{22}$ alloy.[11] Therefore, at temperature below M_s, growth and reorientation of the 10M martensite variant initially occur by tensile loading. Subsequently, by further tensile loading, growth of the 14M martensite and its variant rearrangement occur. These stress- and thermal-induced transformation behaviors are very similar to those of the Ni_2MnGa FSMAs.[16]

Finally, the result of the compressive test in the martensite phase is shown. A single crystal of $Ni_{54.1}Ga_{26.9}Fe_{19}$ alloy with M_s=47.2, M_f=20.0, A_s=25.1, and A_f=56.1 °C was used for the compressive test, where the size of specimen was $3.7\times3.7\times5.0$ mm^3 and the compressive test was carried out at a strain rate 0.5 mm/min at 24 °C, which is just below A_s. Figure 3 shows the compressive stress–strain curve obtained by applying a compressive stress to the direction indicated in the stereographic triangle in Fig. 3(b), where a compressive stress had been previously applied to the direction indicated in the stereo triangle Fig. 3(a) in order to obtain a single-variant structure. In the previous deformation, the compressive stress required for variant reorientation was over 10 MPa. In the second deformation, however, two plateau regions appeared, the stress level of the first plateau being about only 2–3 MPa as shown in Fig. 3. It is supposed that the variant rearrangement of the 14 and/or 10M structure occurred and then the $L1_0$ structure was stress induced from the 14 or 10M structure. This very low compressive stress of about 2–3 MPa is almost the same level as those of the 14 and 10M martensites of the Ni–Mn–Ga alloys.[9]

In conclusion, superelasticity can be obtained in the tensile test above M_s for the $Ni_{54}Ga_{27}Fe_{19}$ alloy. The parent phase with $L2_1$ transforms into the stress-induced martensite phase with 14M by tensile stress and subsequently, the 14M stress-induced martensitically transforms into $L1_0$ by further applying stress. On the other hand, below M_s, the variant rearrangement of the thermally induced martensite phase with the 10M proceeds due to the tensile stress and then the 10–14M stress-induced transformation followed by the 14M–$L1_0$ stress-induced transformation subsequently occurs. Moreover, in the compressive test, the variant rearrangement proceeds by very low compressive stress less than 3 MPa.

The authors wish to thank T. Ota for his help with the experimental work. This study was supported by Grants-in-Aid for Science Research from the Ministry of Education, Science, Sports and Culture, Japan. It was also supported by the Industrial Technology Research Grant Program from the New Energy and Industrial Technology Development Organization (NEDO), Japan.

[1] K. Ullakko, J. K. Huang, C. Kanter, V. V. Kokorin, and R. C. O'Handley, Appl. Phys. Lett. **69**, 1966 (1996).
[2] R. D. James and M. Wutting, Philos. Mag. A **77**, 1273 (1998).
[3] T. Kakeshita, T. Takeuchi, T. Fukuda, T. Saburi, R. Oshima, S. Muto, and K. Kishio, Mater. Trans., JIM **41**, 882 (2000).
[4] F. Gejima, Y. Sutou, R. Kainuma, and K. Ishida, Metall. Mater. Trans. A **30**, 2721 (1999).
[5] A. Fujita, K. Fukamichi, F. Gejima, R. Kainuma, and K. Ishida, Appl. Phys. Lett. **77**, 3054 (2000).
[6] M. Wutting, J. Li, and C. Craciunescu, Scr. Mater. **44**, 2393 (2001).
[7] K. Oikawa, L. Wulff, T. Iijima, F. Gejima, T. Ohmori, A. Fujita, K. Fukamichi, R. Kainuma, and K. Ishida, Appl. Phys. Lett. **79**, 3290 (2001).
[8] H. Morito, A. Fujita, K. Fukamichi, R. Kainuma, K. Ishida, and K. Oikawa, Appl. Phys. Lett. **81**, 1657 (2002).
[9] A. Sozinov, A. A. Likhachev, and K. Ullakko, IEEE Trans. Magn. **38**, 2814 (2002).
[10] D. L. Schlagel, Y. L. Wu, W. Zhang, and T. A. Lograsso, J. Alloys Compd. **312**, 77 (2000).
[11] K. Oikawa, T. Ota, T. Ohmori, Y. Tanaka, H. Morito, A. Fujita, R. Kainuma, K. Fukamichi, and K. Ishida, Appl. Phys. Lett. **81**, 5201 (2002).
[12] K. Oikawa, T. Ota, Y. Sutou, T. Ohmori, R. Kainuma, and K. Ishida, Mater. Trans., JIM **43**, 2360 (2002).
[13] Y. Li, C. Jiang, T. Liang, Y. Ma, and H. Xu, Scr. Mater. **48**, 1255 (2003).
[14] Z. H. Liu, M. Zhang, Y. T. Cui, Y. Q. Zhou, W. H. Wang, G. H. Wu, X. X. Zhang, and G. Xiao, Appl. Phys. Lett. **82**, 424 (2003).
[15] H. Morito, A. Fujita, K. Fukamichi, T. Ota, R. Kainuma, K. Ishida, and K. Oikawa, Mater. Trans., JIM **44**, 661 (2003).
[16] V. V. Kokorin, V. V. Martynov, and V. A. Chernenko, Sov. Phys. Solid State **33**, 708 (1991).
[17] V. A. Chernenko, V. V. Kokorin, O. M. Babii, and I. K. Zasimchuk, Intermetallics **6**, 29 (1998).
[18] T. Saburi and S. Nenno, *Proceedings of the International Conference on Solid-Solid Phase Transformation*, edited by H. I. Aaronson, D. E. Laughlin, R. E. Sekerka, and C. M. Wayman (AIME, New York, 1982), Vol. 1455.
[19] H. Horikawa, S. Ichinose, S. Morii, S. Miyazaki, and K. Otsuka, Metall. Trans. A **19**, 915 (1988).
[20] R. Kainuma, H. Nakano, and K. Ishida, Metall. Trans. A **27**, 4153 (1996).
[21] R. Kainuma, F. Gejima, Y. Sutou, I. Ohnuman, and K. Ishida, Mater. Trans., JIM **41**, 943 (2000).
[22] K. Otsuka, H. Sakamoto, and K. Shimizu, Acta Metall. **27**, 585 (1979).